



**GEOLOGICAL SURVEY OF  
CANADA**

**OPEN FILE 5545**

**ALBERTA ENERGY AND UTILITIES BOARD  
ALBERTA GEOLOGICAL SURVEY**

**SPECIAL REPORT 87**

---

**Chemistry of kimberlite indicator minerals and sphalerite  
derived from glacial sediments of northwest Alberta**

---

**A. Plouffe, R.C. Paulen, I.R. Smith, and I.M. Kjarsgaard**

2007



Natural Resources  
Canada

Ressources naturelles  
Canada

**Canada**

**GEOLOGICAL SURVEY OF CANADA**

**OPEN FILE 5545**

**ALBERTA ENERGY AND UTILITIES BOARD**

**ALBERTA GEOLOGICAL SURVEY**

**SPECIAL REPORT 87**

**Chemistry of kimberlite indicator minerals and  
sphalerite derived from glacial sediments of northwest  
Alberta**

A. Plouffe, R.C. Paulen, I.R. Smith, and I.M. Kjarsgaard

**2007**

©Her Majesty the Queen in Right of Canada 2007

Available from:  
Geological Survey of Canada  
3303 – 33<sup>rd</sup> Street NW  
Calgary, AB  
T2L 2A7

Alberta Geological Survey  
4th floor Twin Atria Building  
4999 – 98th Avenue  
Edmonton, AB  
T6B 2X3

Geological Survey of Canada  
601 Booth St.  
Ottawa, ON  
K1A 0E8

**Plouffe, A., Paulen, R.C., Smith, I.R., and I.M. Kjarsgaard**

**2007: Chemistry of kimberlite indicator minerals and sphalerite derived from glacial sediments of northwest Alberta**, Alberta Energy and Utilities Board, Alberta Geological Survey, Special Report 87, Geological Survey of Canada, Open File 5545, 1 CD-ROM.

Open files are products that have not gone through the GSC formal publication process.

## TABLE OF CONTENT

List of figures .....	4
List of tables.....	5
List of Appendices .....	5
ABSTRACT .....	7
INTRODUCTION .....	8
STUDY AREA: LOCATION AND GEOLOGY .....	8
METHODOLOGY .....	11
<i>Mineral identification</i> .....	12
RESULTS .....	13
<i>Distribution of potential kimberlite indicator minerals</i> .....	13
<i>Kimberlite indicator minerals chemical composition</i> .....	20
<i>Distribution of sphalerite in till</i> .....	26
<i>Chemical composition of sphalerite</i> .....	27
ON-GOING RESEARCH .....	35
SUMMARY .....	36
ACKNOWLEDGEMENTS.....	36
REFERENCES .....	37

## List of figures

1. Location of the study area: NTS map sheets 84L (Zama Lake) and 84M (Bistcho Lake) in northwest Alberta.
2. Regional ice-flow patterns in northwest Alberta, northeast British Columbia and southern Northwest Territories.
3. Glacial sample location map of the Zama Lake (NTS 84L) and Bistcho Lake (NTS 84M) area.
4. (A) Un-normalized number of KIMs in till shown on a topographic map, and (B) on a digital elevation model constructed from the shuttle radar topography mission data (SRTM).
5. (A) Un-normalized number of KIMs in glaciofluvial sediments shown on a topographic map, and (B) on a digital elevation model constructed from the shuttle radar topography mission data (SRTM).
6. Photographs of Cr-pyrope garnet from (A) glaciofluvial sample 3151, and (B) till sample 3205.
7. CaO vs. Cr<sub>2</sub>O<sub>3</sub> for pyrope garnets recovered from till and glaciofluvial sediments.
8. Cr<sub>2</sub>O<sub>3</sub> vs. Al<sub>2</sub>O<sub>3</sub> for all diopsides analyzed.
9. Photograph of olivine (forsterite) from till sample 2252.
10. NiO vs. Fo content (equivalent to Mg number) in olivine.
11. Cr<sub>2</sub>O<sub>3</sub> vs. MgO for all spinels analyzed.
12. Cr<sub>2</sub>O<sub>3</sub> vs. MgO for all Mg-ilmenites analyzed.

13. Number of sphalerite grains normalized to 30 kg till sample weight. Results are depicted on (A) a topographic map base, and (B) a digital elevation model constructed from the shuttle radar topography mission data.
14. Number of galena grains normalized to 30 kg till sample weight. Results are depicted on (A) a topographic map base, and (B) a digital elevation model constructed from the shuttle radar topography mission data.
15. Photographs of sphalerite and galena grains recovered from till samples from NW Alberta.
16. Scanning electron microscope (SEM) backscatter images of sphalerite grains recovered from till samples.
17. Correlation graphs between (A) Fe and Zn and (B) Zn and Cd in sphalerite.

## **List of tables**

1. Kimberlite indicator mineral abundance in the three most anomalous samples.
2. Average and standard deviation of the Zn, Fe, and Cd concentrations in the sphalerite core and grain periphery (grain corner) from this study compared with data from the Pine Point deposit (Kyle, 1981).

## **List of Appendices**

1. Sample location information and kimberlite indicator mineral counts.
2. Electron microprobe data for pyrope garnet.
3. Electron microprobe data for diopside.<sup>4</sup>
4. Electron microprobe data for olivine.

5. Electron microprobe data for chromite or Cr-spinel.
6. Electron microprobe data for Mg-ilmenite.
7. Electron microprobe data for of corundum.
8. Electron microprobe analyses of rutile.
9. Revised estimated number of sphalerite and galena grains from till samples from NW Alberta.
10. (A) Scanning electron microscope backscatter images of the polished sections of sphalerite grains submitted for electron microprobe analyses; (B) electron microprobe analyses of sphalerite.
11. Quality assurance and quality control data for the sphalerite electron microprobe analyses.

## **Abstract**

Plouffe et al. (2006a) reported the presence of kimberlite indicator minerals (KIMs), and sand-sized sphalerite and galena grains in glacial sediments from northwest Alberta. In this report most of the KIMs, originally identified from optical properties alone, are now confirmed as such following detailed electron microprobe analyses. The exceptions to this are 1) fifteen grains originally classified as low Cr-diopside that are re-interpreted as KIMs because their  $\text{Cr}_2\text{O}_3$  content exceeds 0.5 wt.%, and 2) one grain originally identified as chromite is re-classified as crustal ilmenite. These new results confirm the presence of anomalous concentrations of KIMs in three glacial sediment (till) samples and suggest that an unknown kimberlitic source is reflected in the glacial sediments of northwest Alberta. Electron microprobe analyses (n=180) were completed on 15 sphalerite grains recovered from till in the region of the sphalerite anomaly (Plouffe et al., 2006a). The sphalerite grains have an average composition of 33.4 wt.% S, 65.4 wt.% Zn, 0.7 wt.% Fe, 0.43 wt.% Cd, and trace amounts (0.3 to 0.1 wt.%) of Cu, Ag, Se, and In which is slightly different from the sphalerite from the Pine Point deposit.

## ***Introduction***

The presence of a limited number of potential kimberlite indicator minerals (KIMs) and anomalous concentrations of sphalerite grains in till in northwest Alberta was presented in a joint publication of the Geological Survey of Canada and the Alberta Geological Survey (Plouffe et al., 2006a). This report was released in an expeditious manner in order to benefit the mineral exploration industry in Alberta. Following the release of the report, a large part of the ground, in the region of the sphalerite anomaly and where potential KIMs were also reported, was staked (Alberta Energy, 2006 - <http://www.energy.gov.ab.ca/2741.asp>). The purpose of this new Open File is to present the results of electron microprobe analyses conducted on the potential kimberlite indicator minerals and the sphalerite grains reported in Plouffe et al. (2006a). These data confirm that the potential kimberlite indicator minerals, identified from optical properties alone, indeed have a chemical composition that could be linked to a kimberlitic source. Furthermore, the chemistry of a number of kimberlite indicator minerals provides some indication on the composition of the magma sampled by kimberlites and can be used to establish and to predict the diamond potential of their source rock (see for e.g. Dawson and Stephens, 1975; Haggerty, 1975; Nimis, 1998; Grütter et al., 2004; Wyatt et al., 2004).

This research was conducted as part of a four year collaborative project (2003-2007) between the Alberta Geological Survey, the British Columbia Ministry of Energy, Mines and Petroleum Resources and the Geological Survey of Canada (GSC). The project is entitled Shallow Gas and Diamond Opportunities in Northern Alberta and British Columbia and is being conducted as part of the Northern Resources Development Program of the GSC. As stated in the title of the project, one of its objectives is to define the potential of northwest Alberta to host diamondiferous kimberlites.

## ***Study area: location and geology***

The study area as defined in this report extends over the Zama Lake (NTS 84L) and Bistcho Lake (NTS 84M) map areas in northwest Alberta, directly adjacent to the Northwest Territories and British Columbia boundaries (Fig. 1). It lies within the Fort

Nelson Lowlands of the Alberta Plateau physiographic region (Bostock, 1967) which is a region of subdued to flat relief with an elevation varying from 350 m to 550 m above sea level (asl) except for isolated hills such as the Cameron Hills which reach a maximum elevation of 760 m asl.



**Figure 1.** Location of the study area: NTS map sheets 84L (Zama Lake) and 84M (Bistcho Lake) in northwest Alberta.

Because of its flat nature, and the low permeability of the surface sediments, the region is poorly drained and organic deposits in the form of bogs and fens are very abundant.

The regional bedrock and glacial geology are discussed in Plouffe et al. (2006a) and is herein summarized only briefly. The bedrock geology consists of nearly horizontal and poorly indurated Cretaceous Shaftesbury Formation shale overlain by Cretaceous

Dunvegan Formation sandstone (Okulitch, 2006) at an elevation of approximately 700 m asl. Bedrock outcrops are rare and have been encountered in meltwater channels, along modern stream valleys, and on hilltops. Outcrops are indicated on the surficial geology maps produced as part of this collaborative project: (Plouffe et al., 2004, 2006b; Paulen et al., 2005a, 2005b, 2006a, 2006b; Smith et al., 2005b, in press; Kowalchuk et al., 2006).

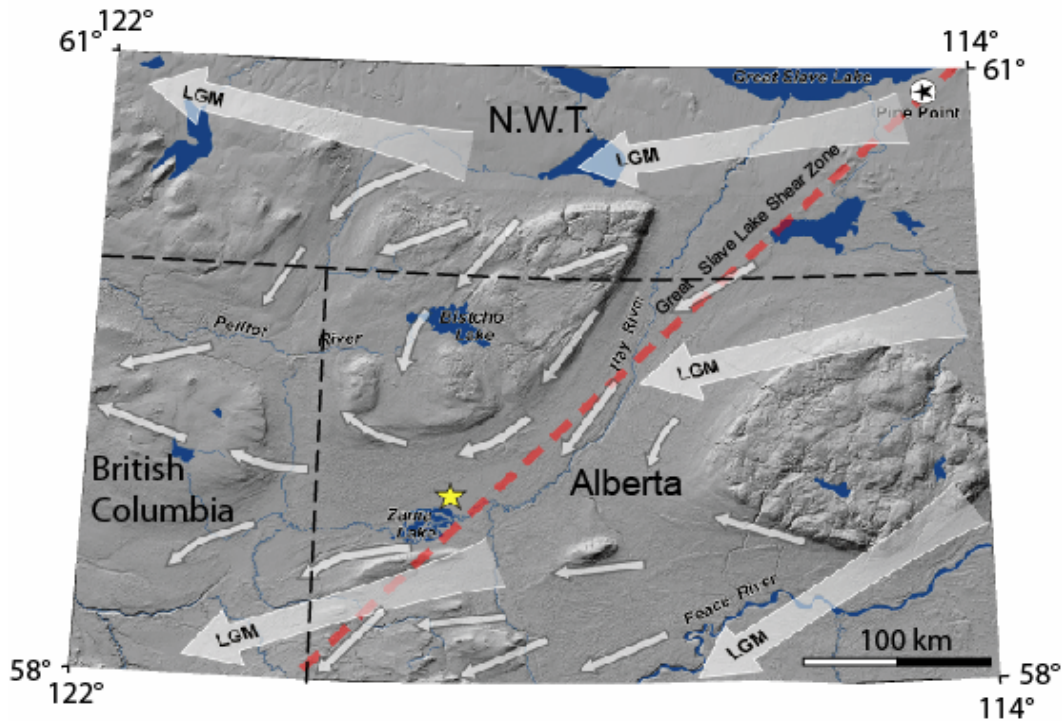


**Figure 2.** Regional ice-flow patterns in northwest Alberta, northeast British Columbia and southern Northwest Territories. Large arrows depict regional ice flow during the Last Glacial Maximum (LGM) and small arrows depict ice movements during deglaciation. The yellow star indicates the location of a sphalerite anomaly in glacial sediments reported by Plouffe et al. (2006a). Red dashed line indicates the location of the Great Slave Lake Shear Zone.

The region is covered by an extensive cover of glacial sediments which varies greatly in thickness from 0 to 450 m (Pawlowicz et al., 2005a, 2005b, in press-a, in press-b). During the Late Wisconsinan glaciation, ice derived from the Keewatin Sector of the Laurentide Ice Sheet flowed west and southwest across the area (Fig. 2). Ice-flow direction indicators are limited to the macro-landforms observed on air photos and digital elevation models, and from a limited number of till clast fabrics measured during field

activities. Bedrock striations common in the Canadian Shield are absent in this region because of the poorly indurated nature of the local shale and sandstone bedrock. Local ice-flow directions are visible on the aforementioned surficial geology maps. During ice retreat, which occurred from 11 500 to 11 000 radiocarbon years before present (equivalent to 13 450 to 13 000 calendar years before present) (Dyke, 2004), glacial lakes developed over a large sector of the region because of the damming of the eastward drainage by ice. Consequently, glacial lake sediments overlie till in the lowest sector of the Hay River drainage basin. Future mineral exploration follow-up activities in this region relying on drift prospecting should take into consideration the distribution of glacial lake sediments because they represent a serious impediment for till sampling where they reach a thickness greater than one meter. Glaciofluvial sand and gravel have been deposited in some meltwater channels and at the outlets of glacial lakes (Mathews, 1980; Smith et al., 2005a). Sampling of glaciofluvial sediment for drift exploration is possible in this region but would be restricted by its scarce distribution.

## ***Methodology***

Details on field sampling methods and laboratory procedures for heavy mineral separation and identification are presented in Plouffe et al. (2006a). Plouffe et al. (2006a) reported the presence of potential kimberlite indicator minerals including forsterite, Cr-diopside, Mg-ilmenite, pyrope, and chromite recovered from ca 30 kg till and glaciofluvial sediments within the study area. The potential KIMs and other minerals of interest were isolated from the nonferromagnetic heavy mineral concentrates at Overburden Drilling Management Ltd. (ODM), Nepean, Ontario. All potential KIMs plus grains of crustal ilmenite, Cr-diopside, rutile, zircon, corundum, and diaspore were mounted on 5 mm thick resin epoxy stubs and then polished to expose a cross-section of the minerals at SGS Lakefield Research Ltd. During the first part of this process, 3 grains were lost (2 pyropes and 1 chromite; see Appendix 1). It is uncertain whether the grains were lost during the picking or the grain mounting. Scanning electron microscope (SEM) backscatter images were provided by SGS Lakefield Research Ltd. to identify individual grains. Mineral analyses were performed by I.M. Kjarsgaard on a four-spectrometer wavelength dispersive CAMECA Camebax Electron Microprobe at Carleton University,

Ottawa. Overlap corrections were performed using the PAP procedure. Calibrations were checked by analyzing known USNM standards (not used for calibration) as samples. Oxides were analyzed at 25 kV and 26 to 30 nA with 10 to 20 seconds counting time. Standards used were MgAl<sub>2</sub>O<sub>4</sub> for Mg and Al, Cr<sub>2</sub>O<sub>3</sub> for Cr, MnTi for Mn, CaSiO<sub>3</sub> for Si and Ca, FeTiO<sub>3</sub> for Ti and Fe, NiO for Ni, ZnAl<sub>2</sub>O<sub>4</sub> for Zn, and V for V. Silicates were analyzed at 15kV and 20 nA with counting times of 20 seconds per element. Standards used were: CaSiO<sub>3</sub> for Si and Ca, MgAl<sub>2</sub>O<sub>4</sub> for Al, Mg<sub>2</sub>SiO<sub>4</sub> for Mg, Fe<sub>2</sub>SiO<sub>4</sub> for Fe, Cr<sub>2</sub>O<sub>3</sub> for Cr, MnTi for Ti and Mn, NiO for Ni, KAl<sub>3</sub>Si<sub>3</sub>O<sub>8</sub> for K, NaAl<sub>3</sub>Si<sub>3</sub>O<sub>8</sub> for Na, and ZnAl<sub>2</sub>O<sub>4</sub> for Zn.

One hundred and eighty electron microprobe analyses were conducted on fifteen dark grey to black sphalerite grains from till samples 2930 and 2933 (Plouffe et al., 2006a). The sphalerite grains were randomly selected from the picked grains. The grains were mounted on epoxy stubs, polished, and analysed at SGS Lakefield Research Ltd. The analyses were conducted with a JEOL 733 Superprobe using an accelerating voltage of 30 kV, a cup electron beam of 30 nA, and a measuring time of 20 seconds. Triplicate analyses were used for quality assurance. Microprobe calibration was completed with mineral standards from CANMET and SPI Supplies including chalcopyrite (Cu K $\alpha$  measured with the LiF crystal), arsenopyrite (As L $\alpha$  measured with the TAP crystal), galena (Pb L $\alpha$  measured with the PET crystal), synthetic AgBiSe<sub>2</sub> Cabri-499 (Ag L $\alpha$  measured with the PET crystal), sphalerite (Zn L $\alpha$  measured with the TAP crystal), pyrrhotite Cabre-241 (Fe K $\alpha$  measured with the LiF crystal), greenokite (Cd L $\alpha$  measured with the PET crystal), hertzenbergite (Sn L $\alpha$  measured with the PET crystal), synthetic GaAs (Ga L $\alpha$  measured with the TAP crystal), pure indium metal (In L $\alpha$  measured with the PET crystal), and synthetic TlBrI (Tl L $\alpha$  measured with the LiF crystal).

### **Mineral identification**

Minerals were labelled based on chemical composition. In some cases where not all constituting elements were covered by the analytical routine used, the energy dispersive spectrum (EDS) was checked for additional elements (e.g., for Ba, Sr, Zr in lindsleyite).

Non-stoichiometric alteration products of ilmenite were labelled "FeTi-oxides or TiFe-oxides." AlOOH was labelled diaspore, although it might very well be boehmite.

The thresholds for mineral names used are Cr-diopside:  $>0.5$  wt.%  $\text{Cr}_2\text{O}_3$ , Cr-pyrope:  $>2$  wt.%  $\text{Cr}_2\text{O}_3$ , Mg-Almandine:  $>5$  wt.% MgO and  $<22$  wt.% FeOtot. Garnet classification is based on Grütter et al. (2004). Cr-spinel is the label given spinels with mole fractions of  $\text{Al}_2\text{O}_3 > \text{Cr}_2\text{O}_3$ , whereas chromite has  $\text{Al}_2\text{O}_3 < \text{Cr}_2\text{O}_3$ .

## **Results**

### **Distribution of potential kimberlite indicator minerals**

Appendix 1 contains a list of the samples processed for heavy mineral analysis along with their location information (latitude, longitude, easting, and northing; NAD 83), the sediment type from which the heavy minerals were recovered (till and glaciofluvial sediments), and the number, type, and size of the KIMs. The sample distribution within the study area is depicted on Figure 3.

Potential KIMs were identified in 38 out of 67 samples processed for heavy mineral separation and identification (Figs. 4 and 5, and Appendix 1). The number of KIMs reported herein are slightly different than the ones in Plouffe et al. (2006a) because 1) 15 grains identified as low Cr-diopsides from optical properties alone have yielded  $\text{Cr}_2\text{O}_3$  contents higher than 0.5 wt.% indicating that they could be derived from a kimberlitic source and 2) one grain originally identified as chromite was re-classified as crustal ilmenite based on the electron microprobe analysis (see below for details). Three samples are considered to contain anomalous numbers of KIMs with 6, 7, and 9 KIMs (Table 1). The remaining 35 samples contain 1 to 3 indicator grains which are dominantly pyrope and chromite with lesser amounts of forsterite, Mg-ilmenite, and Cr-diopside (Figs. 4 and 5). Most of these minerals were recovered in the 0.25 to 0.5 mm size fraction but a limited number of grains were found in the 0.5 to 1 mm size range (Appendix 1). No potential KIMs were detected in the 1 to 2 mm size fraction.

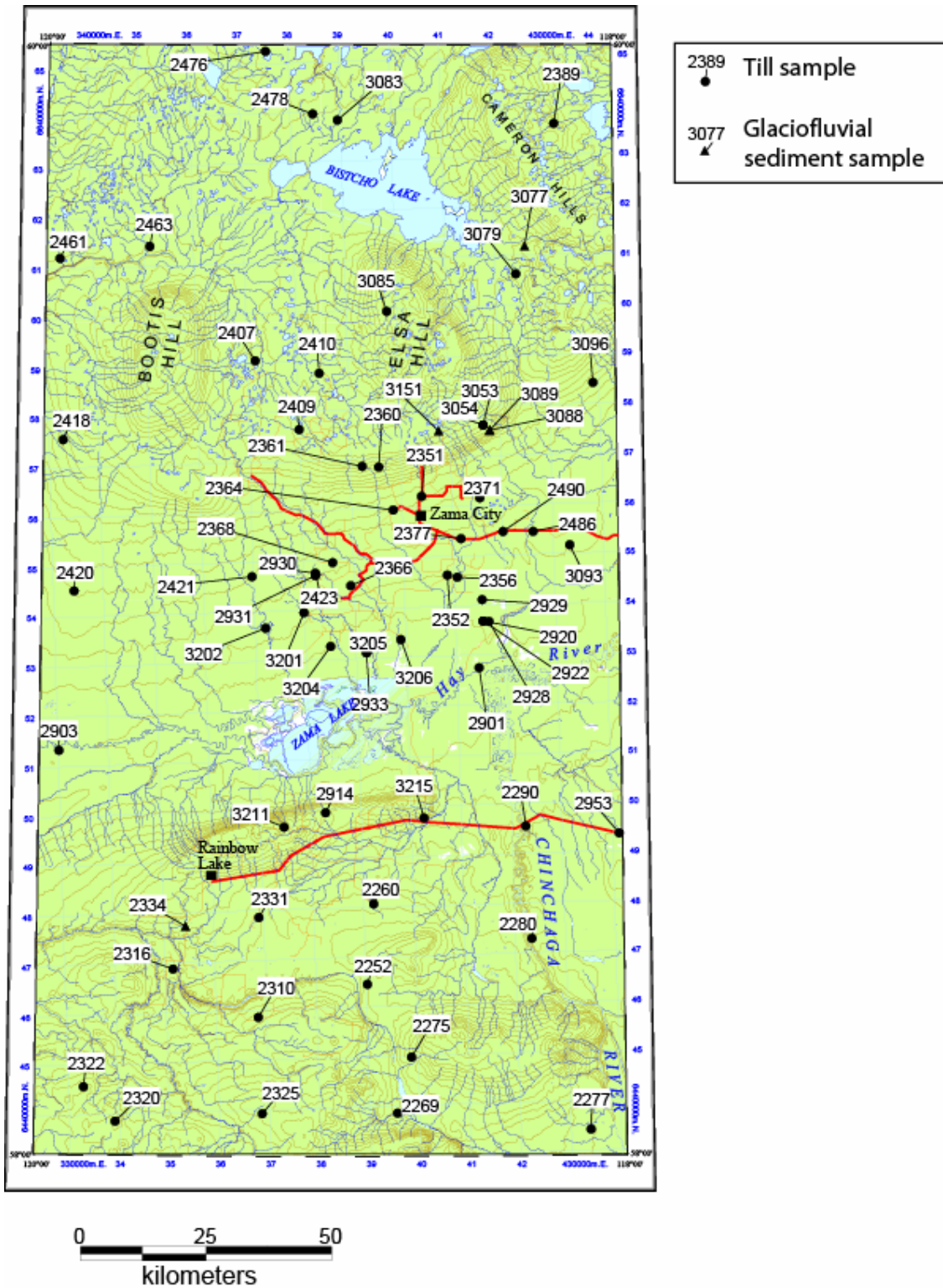


**Figure 3.** Glacial sample location map of the Zama Lake (NTS 84L) and Bistcho Lake (NTS 84M) area.

Sample ID	KIMs	Normalized KIMs (per 30 kg)
2421 (till)	1 pyrope, 3 chromite, 1 forsterite, 2 Cr- diopside	1 pyrope, 3 chromite, 1 forsterite, 2 Cr- diopside
2252 (till)	6 forsterite	8 forsterite
3206 (till)	3 pyrope, 1 Cr- diopside, 2 ilmenite, 1 chromite, 2 forsterite	3 pyrope, 1 Cr- diopside, 2 ilmenite, 1 chromite, 2 forsterite

**Table 1.** Kimberlite indicator minerals in the three most anomalous samples.

A large percentage of the till samples with KIMs are located in the region north of Zama and Hay lakes and south of Elsa Hill, south of Bistcho Lake (Fig. 4). Furthermore, two of the anomalous samples (2421 and 3206) are derived from that region. The other anomalous sample (2252) is located in the southern sector of the Zama Lake map area. Only four glaciofluvial sediment samples were processed for KIMs because of the rareness of that sediment type within the study area. Those samples yielded very few KIMs: zero to two (Fig. 5).

The number of KIM grains when normalized to the amount of till processed for heavy mineral separation ('Table feed' weight in Appendix 2 of Plouffe et al., 2006a) are nearly identical to the raw counts because of the small number of KIMs and the low variation in the weight of material processed on the shaking table (Table 1). Consequently, only the un-normalized counts are reported on Figures 4 and 5.

The bedrock source of the KIMs in the glaciofluvial and till samples is unknown. Samples with 1 or 2 KIMs may represent background concentrations for a region located 100's of km from known kimberlites in the Northwest Territories in the general up-ice region. However, samples containing 6 to 9 KIMs are considered anomalous and might reflect the presence of an unknown kimberlite source closer to the study area.

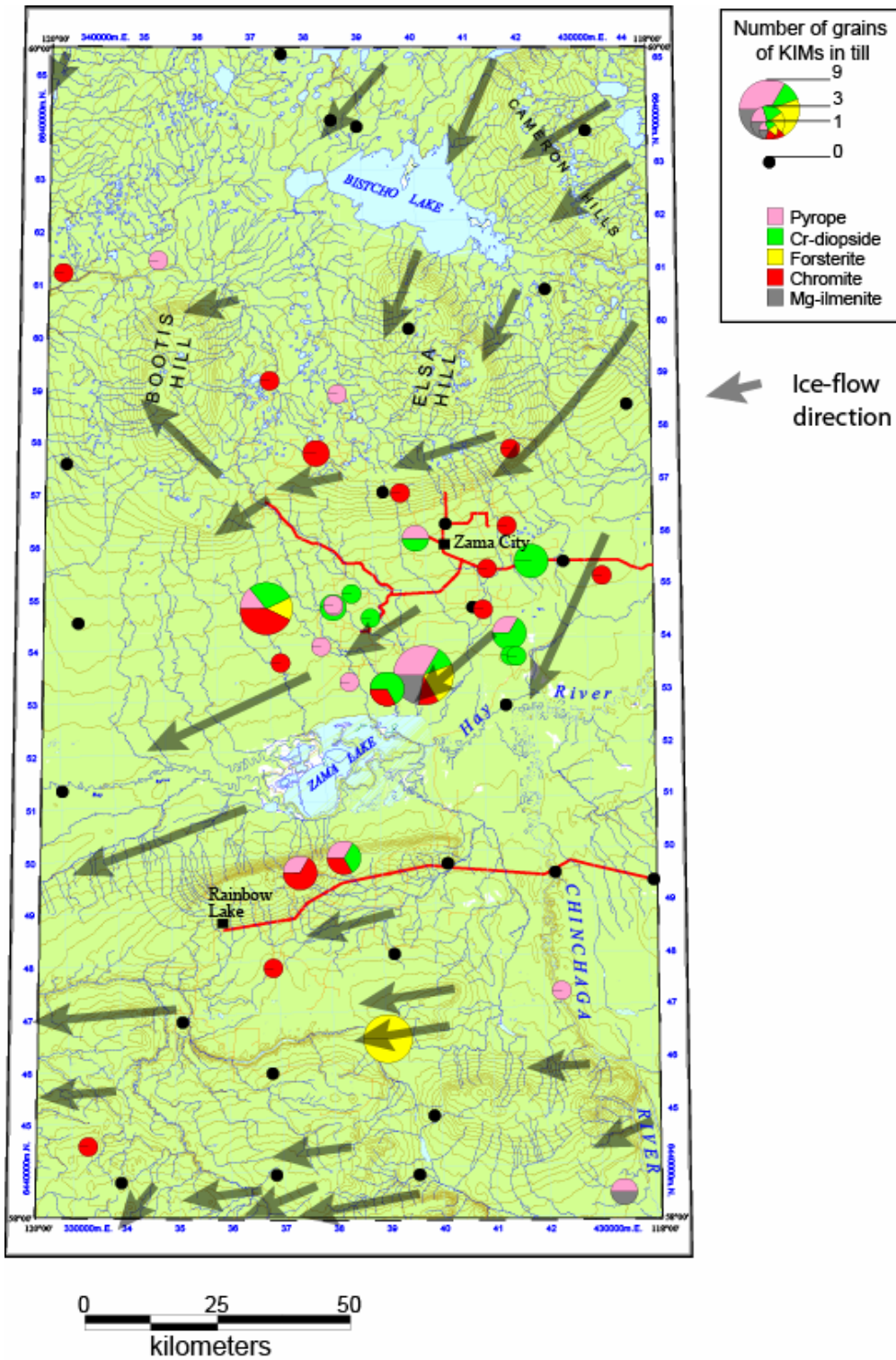


**Figure 4.** (A) Un-normalized number of KIMs in till shown on a topographic map. Ice-flow directions were obtained from the surficial geology maps (Plouffe et al., 2004, 2006b; Paulen et al., 2005a, 2005b, 2006a, 2006b; Smith et al., 2005b, in press).

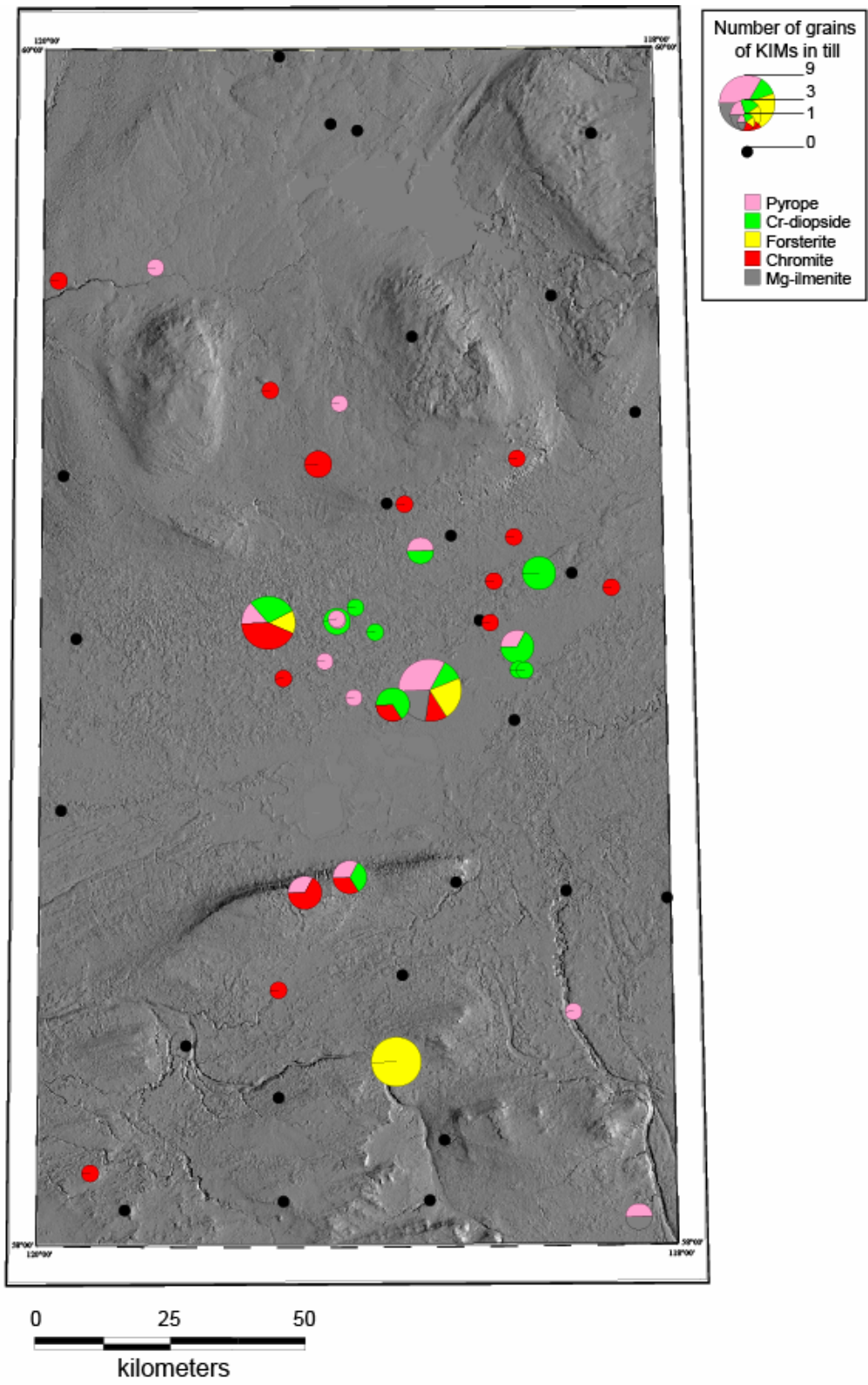


**Figure 4.** (B) Un-normalized number of KIMs in till shown on a digital elevation model constructed from the shuttle radar topography mission data (SRTM).

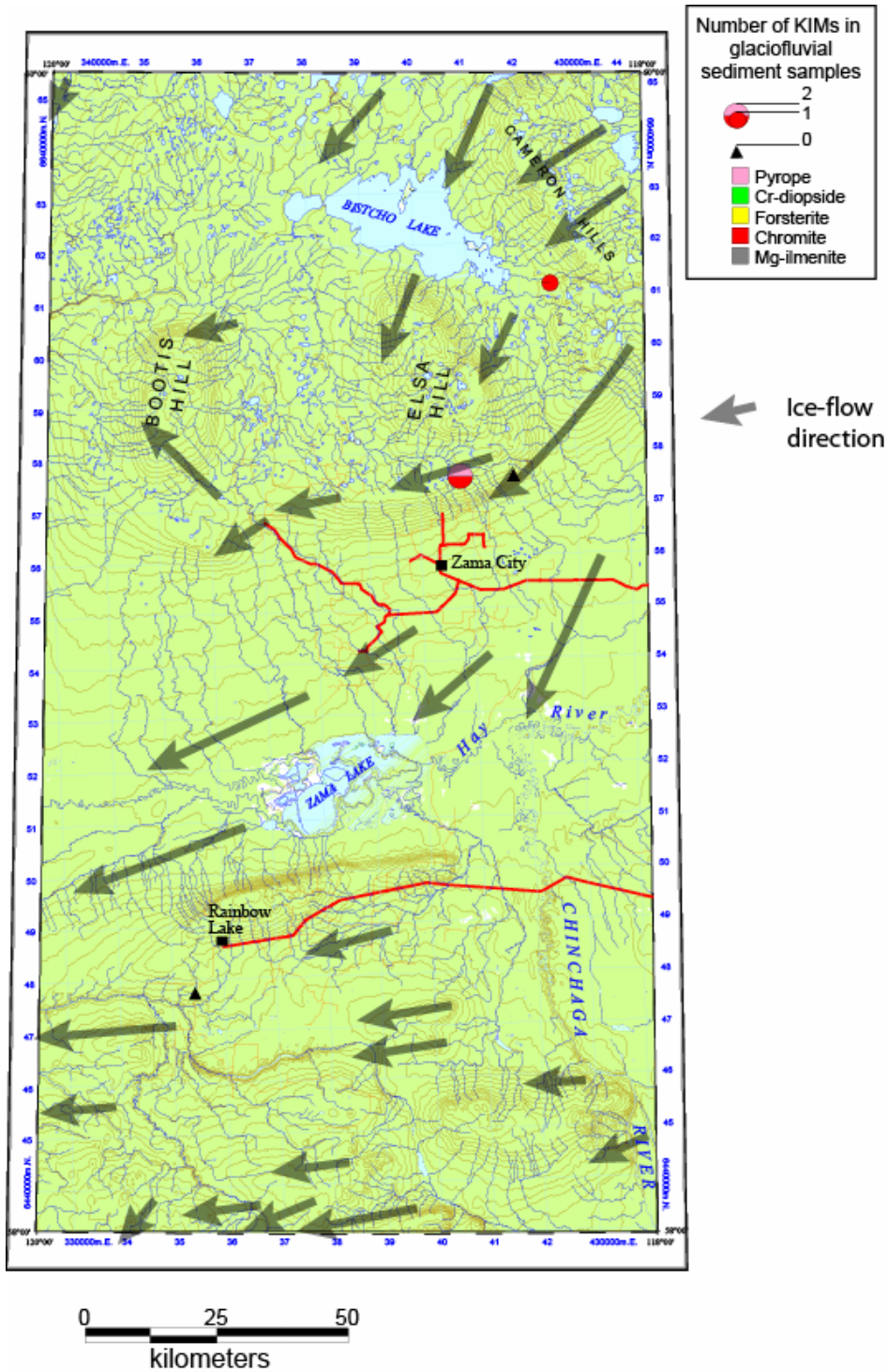


**Figure 5.** (A) Un-normalized number of KIMs in glaciofluvial sediments shown on a topographic map. Ice-flow directions were obtained from the surficial geology maps (Plouffe et al., 2004, 2006b; Paulen et al., 2005a, 2005b, 2006a, 2006b; Smith et al., 2005b, in press).

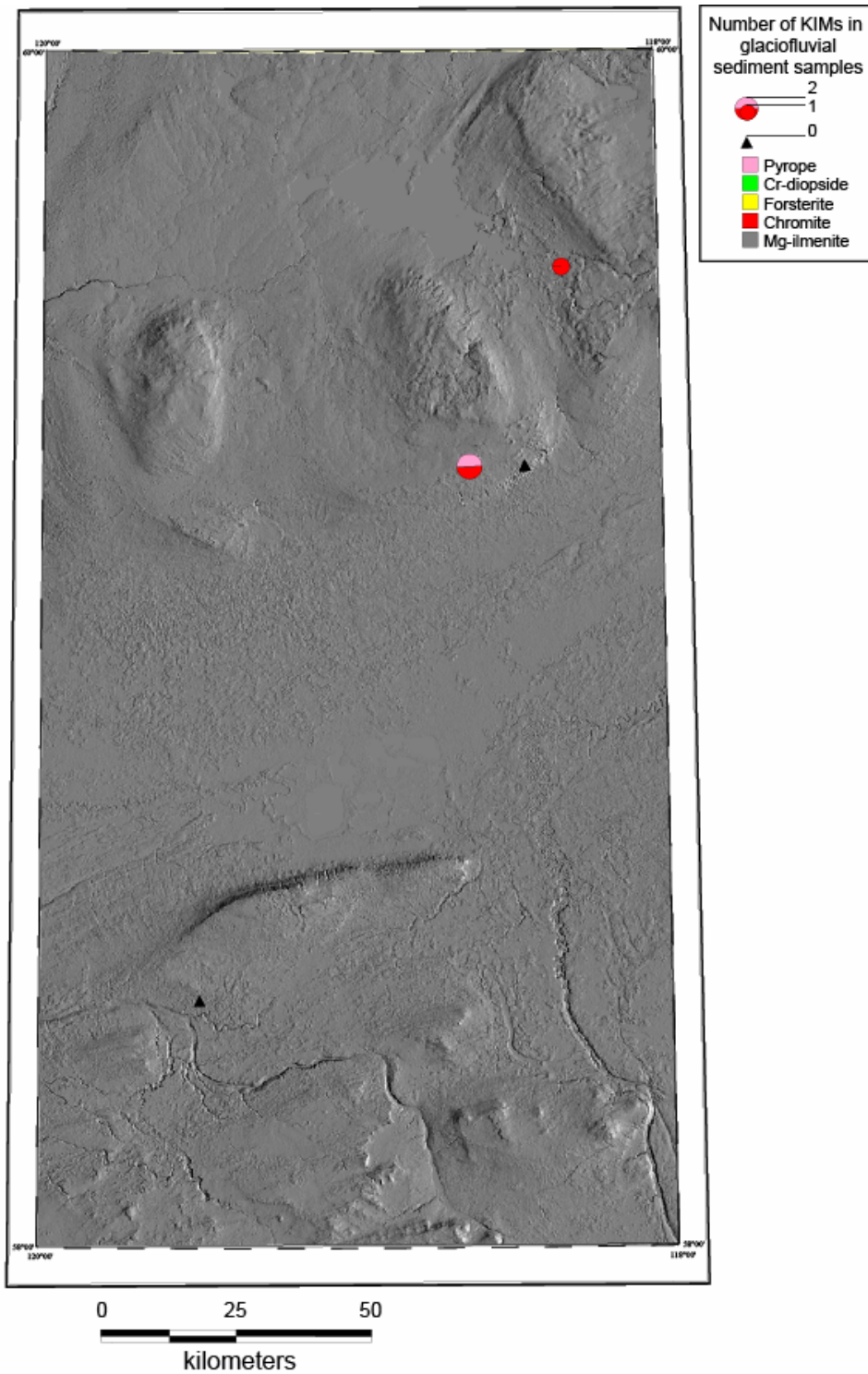


**Figure 5. (B)** Un-normalized number of KIMs in glaciofluvial sediments shown on a digital elevation model constructed from the shuttle radar topography mission data (SRTM).

## Kimberlite indicator minerals chemical composition

**Pyrope Garnet** - A total of 17 Cr-pyrope garnets were analyzed. Mineral chemistry data are presented in Appendix 2. All grains are in the 0.25-0.5 mm size fraction except for two from the 0.5-1.0 mm size range in samples 3205 and 3206 (Fig. 6). The grains are evenly distributed over 15 different samples (Appendices 1 and 2). They contain between 2.46 and 8.01 wt.% Cr<sub>2</sub>O<sub>3</sub> and are mostly from fertile lherzolite (G9; Fig. 7). Two grains, samples 3201 and 2277 contain high TiO<sub>2</sub> (0.77 and 0.98 %, respectively) and close to 4 wt.% Cr<sub>2</sub>O<sub>3</sub> and can be classified as G11 garnets from sheared (or metasomatized) lherzolite. One grain (sample 2463) contains sufficiently high CaO and Cr<sub>2</sub>O<sub>2</sub> to be classified as a wehrlitic garnet (G12) (Fig. 7). No subcalcic harzburgitic or eclogitic garnets were found.



**Figure 6.** Photographs of Cr-pyrope garnet from A) glaciofluvial sample 3151, and B) till sample 3205. Divisions between scale bars = 1 mm.

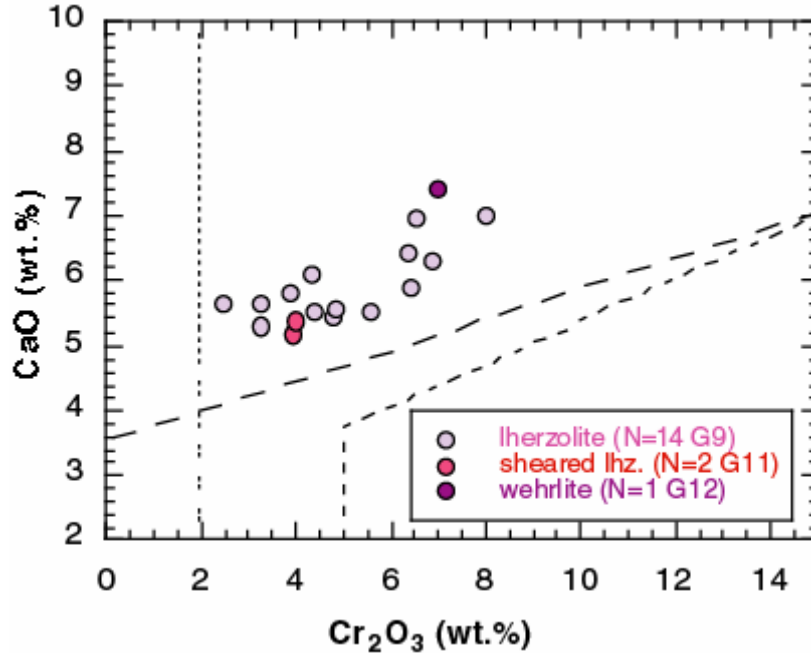


**Figure 7.** CaO vs. Cr<sub>2</sub>O<sub>3</sub> for pyrope garnets recovered from till and glaciofluvial sediments. The long dashed diagonal line represents Gurney's (1984) 85% line essentially dividing Iherzolitic G9 garnets (above) and subcalcic harzburgitic (G10) garnets from diamondiferous assemblages (below). The field starting at 5 wt.% Cr<sub>2</sub>O<sub>3</sub> is Sobolev's (1977) more restricted field for diamondiferous subcalcic harzburgite assemblages. The vertical line at 1 % separates Cr-poor orange garnets of crustal, eclogitic, pyroxenitic or websteritic origin from more Cr-rich peridotitic garnets. Number of G9, G11, and G12 garnets indicated in the legend.

**Diopside** - A total of 42 diopsides were analyzed; results are tabulated in Appendix 3. Diopside grains were all recovered from the 0.25-0.5 mm size fraction with the exception of two grains from the 0.5-1.0 mm size range. Eighteen of them are Cr-diopsides with Cr<sub>2</sub>O<sub>3</sub> ranging from 0.55 to 1.96 wt.% and Mg numbers (100\*MgO/MgO + Fe<sub>0</sub>) ranging from 82.2 to 93.5 (Appendix 3). Most of them plot in the garnet-peridotite field of Figure 8 with the three most Al-rich grains falling into the spinel-peridotite field. However, only three of the thirteen grains in the garnet-peridotite field (one in sample 2368 and two grains in 2940) and one in the spinel-peridotite field have Mg numbers high enough (>90; sample 2366) to have originated from mantle assemblages. Following Nimis' (1998) MgO – Al<sub>2</sub>O<sub>3</sub> classification, these three grains having low Al<sub>2</sub>O<sub>3</sub> and MgO content are most likely low pressure diopsides derived from metasomatized garnet-free peridotites. The other diopsides have Mg numbers below 90 and form a continuous series with the

bulk of the low-Cr diopsides. These diopsides are most likely from crustal mafic to ultra-mafic rocks such as layered intrusions, diabase dikes or komatiites, which can have  $\text{Cr}_2\text{O}_3$  contents up to 1.5 wt.%. Several diopsides with almost no  $\text{Cr}_2\text{O}_3$  but high Mg numbers  $>90$  are likely from impure dolomitic marble or skarn (Fig. 8).

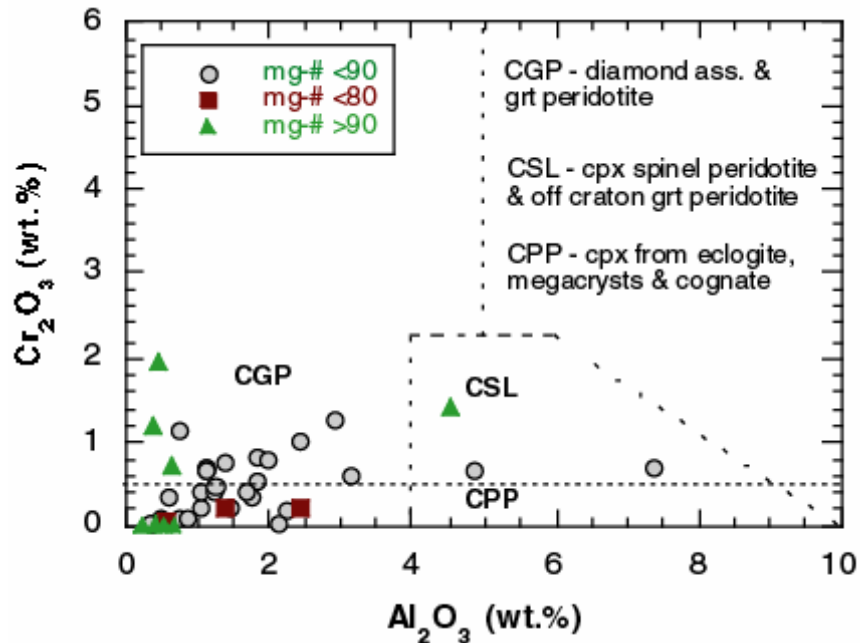


**Figure 8.**  $\text{Cr}_2\text{O}_3$  vs.  $\text{Al}_2\text{O}_3$  for diopsides recovered from till and glaciofluvial sediments. The discriminatory fields are from Nimis (1998); grt – garnet; cpx – clinopyroxene.

Fifteen grains originally reported as low Cr-diopside (approx.  $< 1$  wt.%  $\text{Cr}_2\text{O}_3$ ) by ODM based on optical properties alone (Plouffe et al., 2006a) have yielded  $\text{Cr}_2\text{O}_3$  levels higher than 0.5 wt.% indicating that they could be derived from a kimberlitic source using the criteria established by Nimis (1998). Samples 2364, 2366, 2490, 2914, 2922, 2928, and 3206 each contain one additional Cr-diopside and samples 2929, 2931, and 2933 each contain two additional Cr-diopsides compared to the results reported by Plouffe et al. (2006a) (Appendix 1). These additional grains are herein tabulated as KIMs and are included on Figure 4.

**Olivine-** Olivine was only recovered from three samples: 2252 (n=6), 3206 (n=2) and 2421 (n=1). Olivine is colorless and was difficult to discriminate from other colorless heavy minerals (R. Huneault, Overburden Drilling Management Ltd., personal

communication, 2006) (Fig. 9). Electron microprobe analyses of olivine are presented in Appendix 4. Samples 2252 and 3206 contain olivine in both the 0.25-0.5 mm and the 0.5-1 mm size fraction. All olivine grains analyzed plot into the compositional field of peridotitic olivine and/or kimberlitic megacryst olivine (Fig. 10) with Fo numbers varying from 89 to 93 and NiO values ranging from 0.28 to 0.43 wt.%.

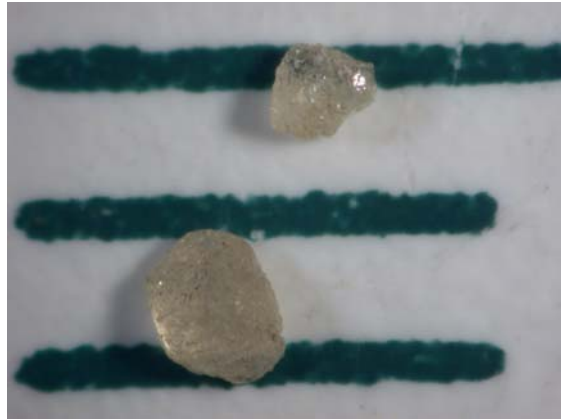


**Figure 9.** Photograph of olivine (forsterite) from sample 2252. Divisions between bars = 1 mm.

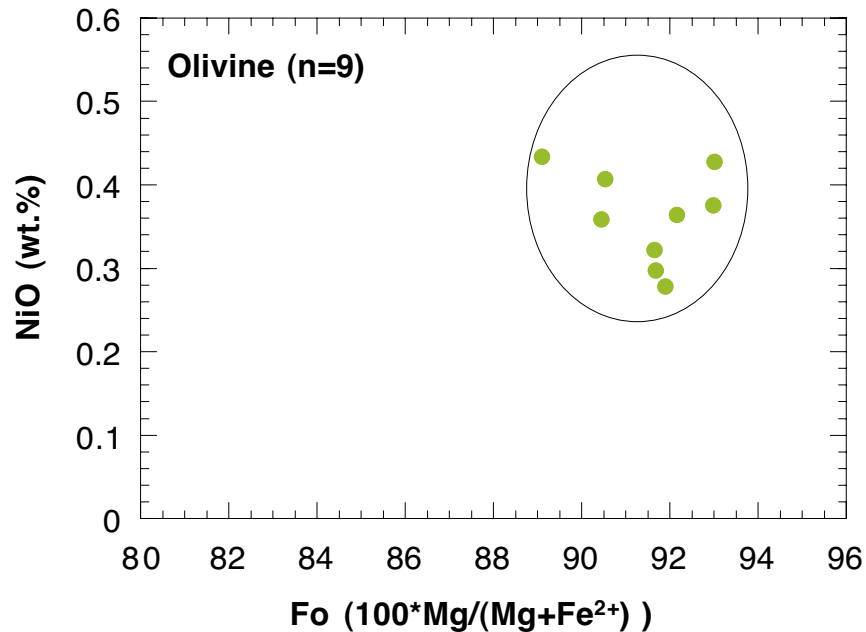


**Figure 10.** NiO vs. Fo content (equivalent to Mg number) for olivine recovered from till samples. The circle outlines the field of typical compositions of peridotitic mantle and kimberlite megacryst olivines.

**Chromite (spinel)** - Twenty four oxide grains consisting of chromite or Cr-spinel were analyzed (Appendix 5). They have widely variable compositions ranging from chromite to chromian hercynite ((Fe,Mg, Cr)Al<sub>2</sub>O<sub>4</sub>) with Cr<sub>2</sub>O<sub>3</sub> levels varying from 20.1 to 51.8 wt.% and MgO from 3.63 to 16.86 wt.%. One grain contained >45 wt.% FeOtot indicating solid solution towards magnetite. The more Cr-rich compositions (>40 wt.% Cr<sub>2</sub>O<sub>3</sub>, n=15) correspond to those typical of spinels from garnet peridotite but the more Al-rich Cr-spinels (<40 wt.% Cr<sub>2</sub>O<sub>3</sub>) are likely from spinel peridotite or crustal ultramafic rocks such as ultramafic layered intrusions. None of the chromites are plotting in the diamond inclusion and intergrowth fields from Fipke et al. (1995) (Fig. 11).

One mineral grain in the glaciofluvial sediment sample 3089 was originally identified as chromite based on optical properties alone (Plouffe et al., 2006a) and was re-identified as a crustal ilmenite following the electron microprobe analysis. Consequently, the probe results reveal that sample 3089 contains no kimberlite indicator minerals (Appendix 1).

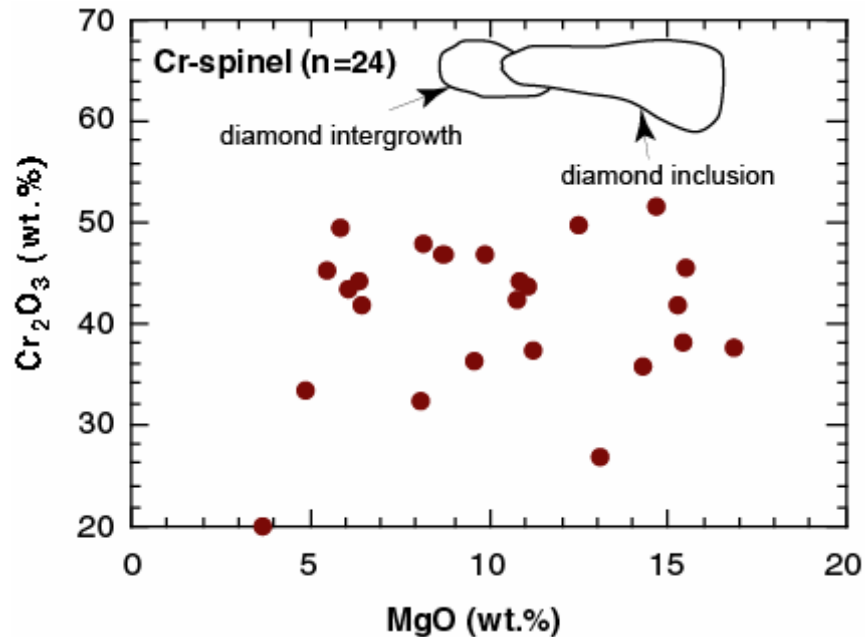


**Figure 11.** Cr<sub>2</sub>O<sub>3</sub> vs. MgO for spinels recovered from till and glaciofluvial samples. The diamond inclusion and intergrowth fields are from Fipke et al. (1995).

**Mg-ilmenite** - Only three of the 91 oxide grains picked as potential ilmenite grains and analyzed are Mg-ilmenite (Appendix 6). They were found in samples 3206 (n=2) and

2277. Samples 3206 and 2277 each contain one grain in the 0.5-1.0 mm size range while the second grain in 3206 is 0.25-0.5 mm in size. The Mg-ilmenite contain between 9.72 and 12.54 wt.% MgO and between 1.26 and 2.06 wt.% Cr<sub>2</sub>O<sub>3</sub> (Fig. 12) and thus fall into the typical compositional range of kimberlitic megacryst ilmenite.

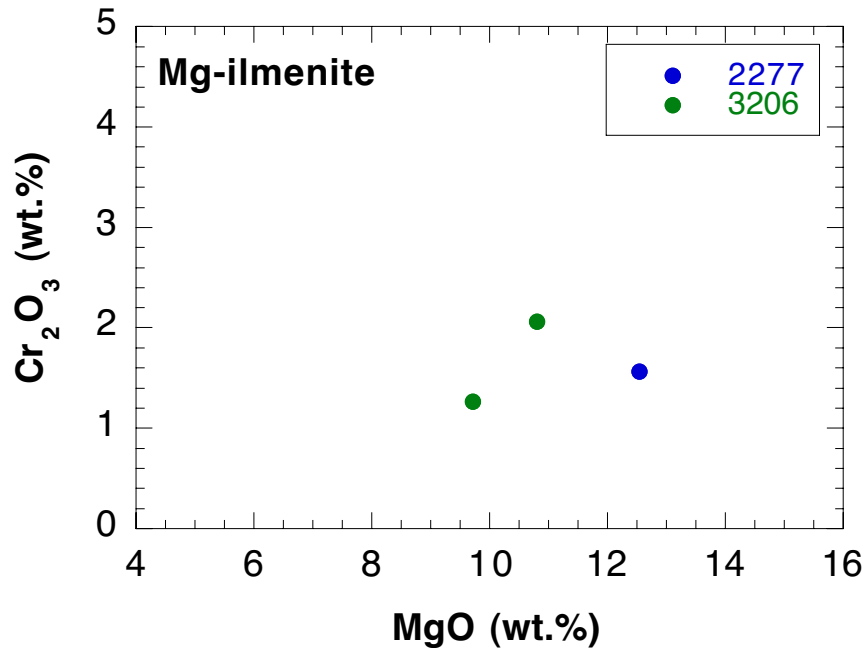


**Figure 12.** Cr<sub>2</sub>O<sub>3</sub> vs. MgO for Mg-ilmenite recovered from till samples.

**Corundum** - Two grains were picked as corundum from the 0.25-0.5 mm size fraction but following electron microprobe analyses one grain from sample 3206 was identified as Al-hydroxide (boehmite or diaspore). The other grain from sample 2931 is true corundum, which contains 0.21 wt.% Cr<sub>2</sub>O<sub>3</sub> and 0.34 wt.% FeOtot (Appendix 7) similar to compositions of pink corundum found in Alberta stream sediments by Friske et al. (2003) and metamorphic ruby compositions compiled by Hutchison et al. (2004).

**Rutile** – Four rutile grains were confirmed as such. Two grains are essentially pure TiO<sub>2</sub> while the other two contain Cr levels varying of 0.56 and 1.10 wt.% which would link them to kimberlites (Appendix 8). Nb<sub>2</sub>O<sub>5</sub> concentrations in the rutile grains are low varying from 0.06 to 1.19 wt.%.

*Non-kimberlitic minerals* – A number of ilmenites initially identified as low-Mg crustal ilmenites based on optical properties were submitted for electron microprobe analyses to characterized variability in ilmenite composition. Analytical results are tabulated in Appendix 6. The grains were found to be crustal ilmenite or their alteration products (non-stoichiometric FeTi-oxides or leucosene). The ilmenite grains contain up to 3.12 wt.% MnO and  $\leq 1.44$  wt.% MgO, several were highly altered to non-stoichiometric FeTi-oxide.

### **Distribution of sphalerite in till**

Plouffe et al. (2006a) reported anomalous concentrations of sphalerite grains with traces of galena recovered from till in a region extending north of Zama Lake to the vicinity of Zama City in northwest Alberta, over NTS map sheets 84L and M (Figs. 13 and 14). Appendix 9 presents the sphalerite and galena abundance data including sample location, total number of sphalerite and galena grains, and the number of sphalerite and galena grains normalized to 30 kg till samples. Most of the recovered sphalerite is dark grey to black and rare grains are of the cleiophane variety (Fig. 15). The grains have angular to sub-angular edges and a few are glacially polished (Figs. 15 and 16). The grains are dominantly from the 0.25 to 0.5 mm size fraction but grains were also recovered from the coarser 0.5 to 1.0 mm and 1.0 to 2.0 mm fractions (Plouffe et al., 2006a). The mineralogical anomaly extends over an area of approximately 1200 km<sup>2</sup> which is interpreted to represent part of a sphalerite dispersal train where the background contents of sphalerite and galena in surrounding regions are zero. One to nine grains of galena were reported in some of the till samples obtained from the anomalous region (Fig. 14). The galena grains are angular to sub-angular and most have a cubic crystal form (Fig. 15). The galena grains were recovered from the 0.25 to 0.5 mm and 0.5 to 1.0 mm size fractions (Plouffe et al., 2006a). Within the sphalerite dispersal train, Zn levels in the silt and clay-sized fraction (<0.063 mm) of till are slightly elevated compared to the surrounding regions but are not considered to be anomalous concentrations (Plouffe et al., 2006a). Furthermore, no significant Pb enrichment was observed in the silt and clay-sized fraction (Plouffe et al., 2006a). None of the five glaciofluvial sediment samples from the study area processed for heavy minerals contain sphalerite or galena. The bedrock source

of the sphalerite and galena grains in till is unknown. The mineralogical anomaly is not thought to be derived from the world class Pine Point deposit located on the south shore of Great Slave Lake (330 km to the northeast) because of the great distance of glacial transport that this would imply and the observed very high sphalerite grain concentrations in till (up to 1200 grains in a 34 kg till sample; Appendix 9). Furthermore, the pristine and fragile nature of the sphalerite and galena grains (Figs. 15, 16 and Appendix 10A) suggests a short glacial transport distance. Consequently, the mineralogical anomaly in till likely points to an undiscovered sedimentary hosted Zn deposit(s).

To identify and characterize the bedrock source of the sphalerite and galena in till, Pb and S isotopic analyses are currently being conducted on selected sphalerite and galena grains. During the process of isolating all sphalerite and galena from the heavy mineral concentrates, the original estimate of the number of sphalerite grains reported by Plouffe et al. (2006a) was reviewed (Appendix 9) because of the greater amount of time spent counting and picking the sphalerite and galena. These new estimates have been used for plotting the maps in Figure 13.

### **Chemical composition of sphalerite**

Fifteen sphalerite grains arbitrarily selected from two samples (2930 and 2933) were submitted for electron microprobe analyses. Polished sections of the sphalerite grains analyzed by electron microprobe are depicted in Appendix 10A to show the general form of the grains most of them showing angular edges. A total of 180 analyses were conducted on grain cores and rims to verify the potential composition variability within single grains. The results are presented in Appendix 10B. Quality assurance and quality control data are provided in Appendix 11. The purpose of these analyses, conducted on a limited number of sphalerite grains, was to confirm the mineralogical identification of sphalerite based on optical properties and to provide quantitative analyses of the sphalerite composition.

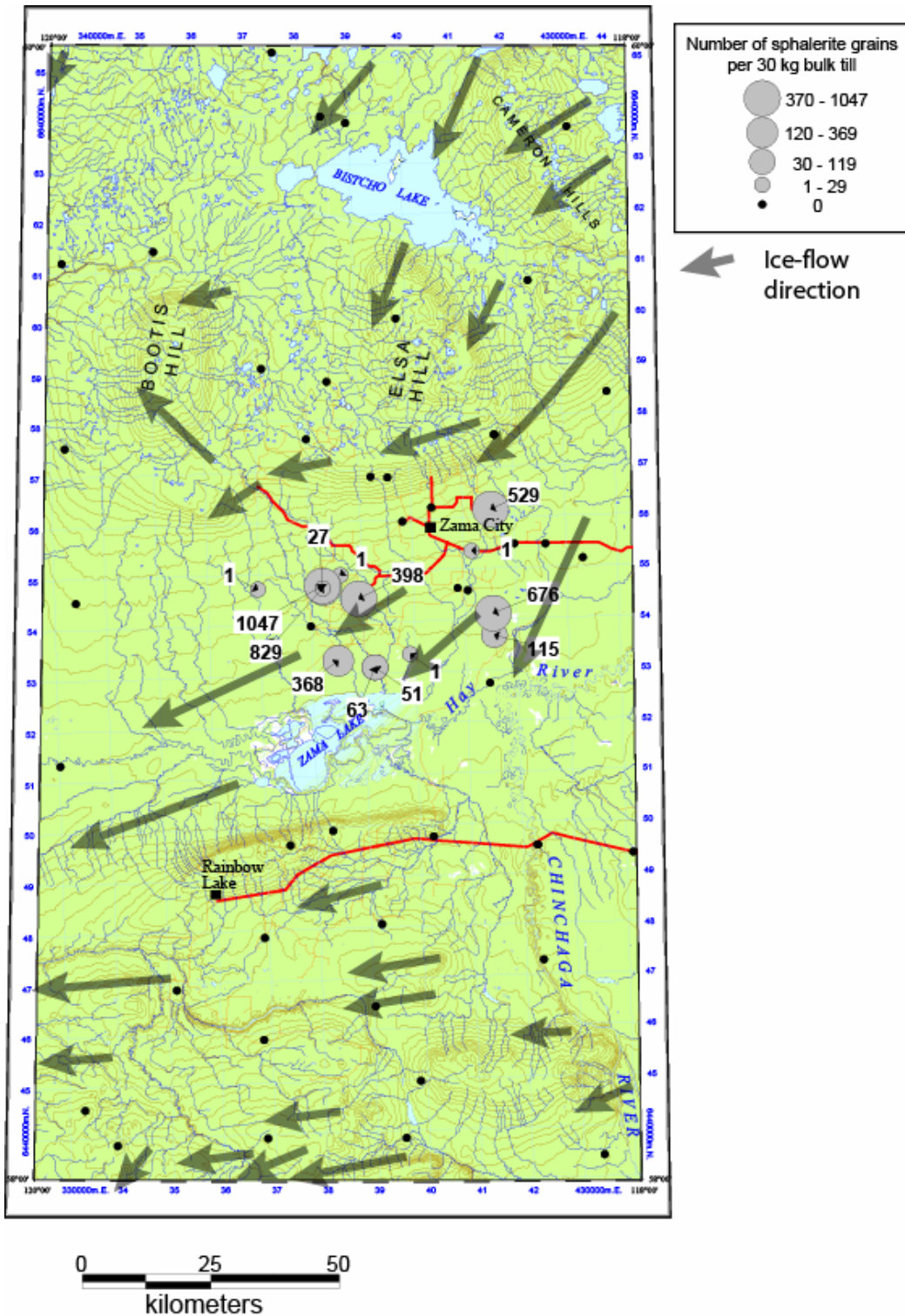


**Figure 13.** (A) Number of spherulite grains normalized to 30 kg till sample weight. Results are depicted on a topographic map base. Ice-flow directions were obtained from the surficial geology maps (Plouffe et al., 2004, 2006b; Paulen et al., 2005a, 2005b, 2006a, 2006b; Smith et al., 2005b, in press).

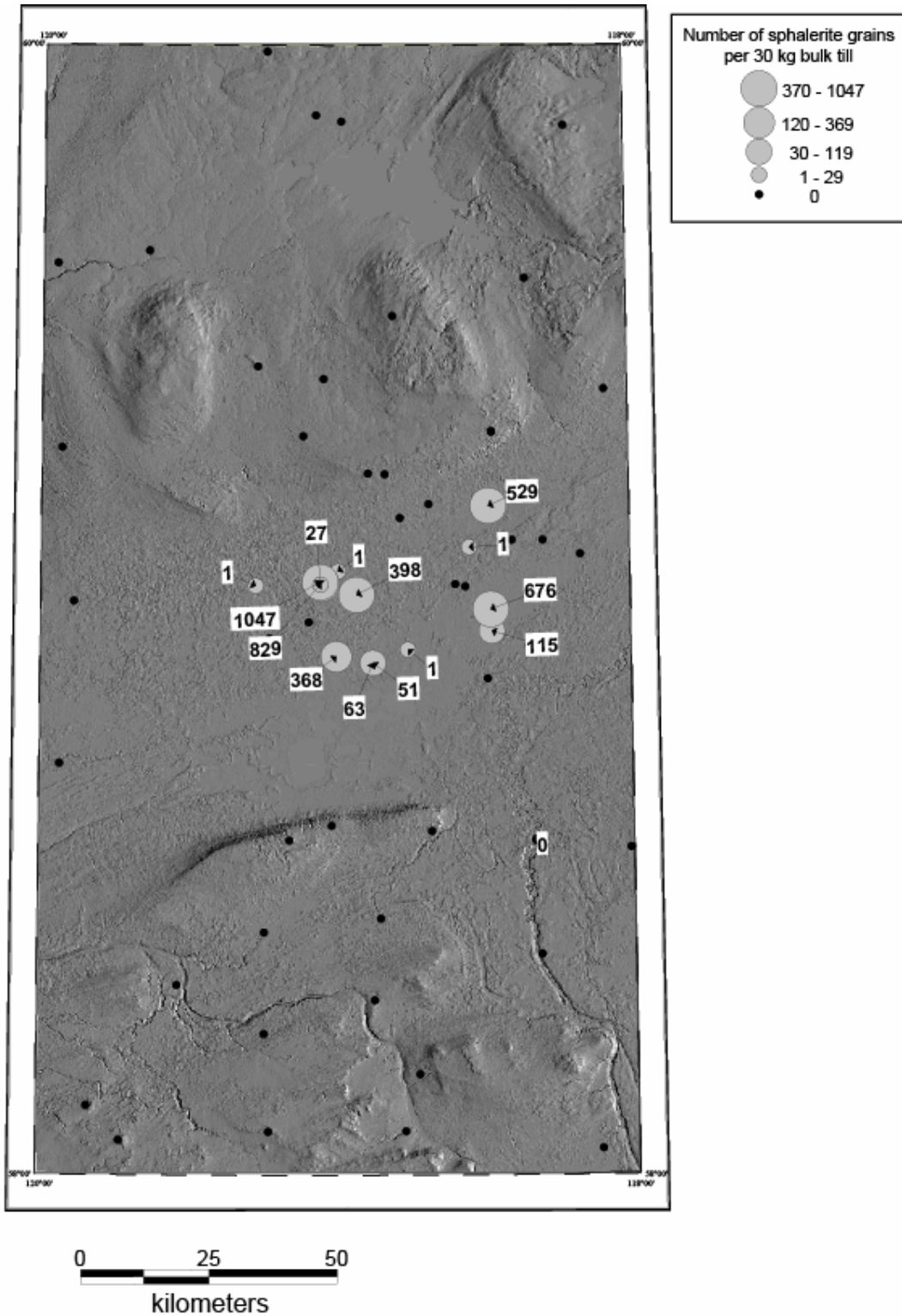


**Figure 13.** (B) Number of sphalerite grains normalized to 30 kg till sample weight. Results are depicted on a digital elevation model constructed from the shuttle radar topography mission data.

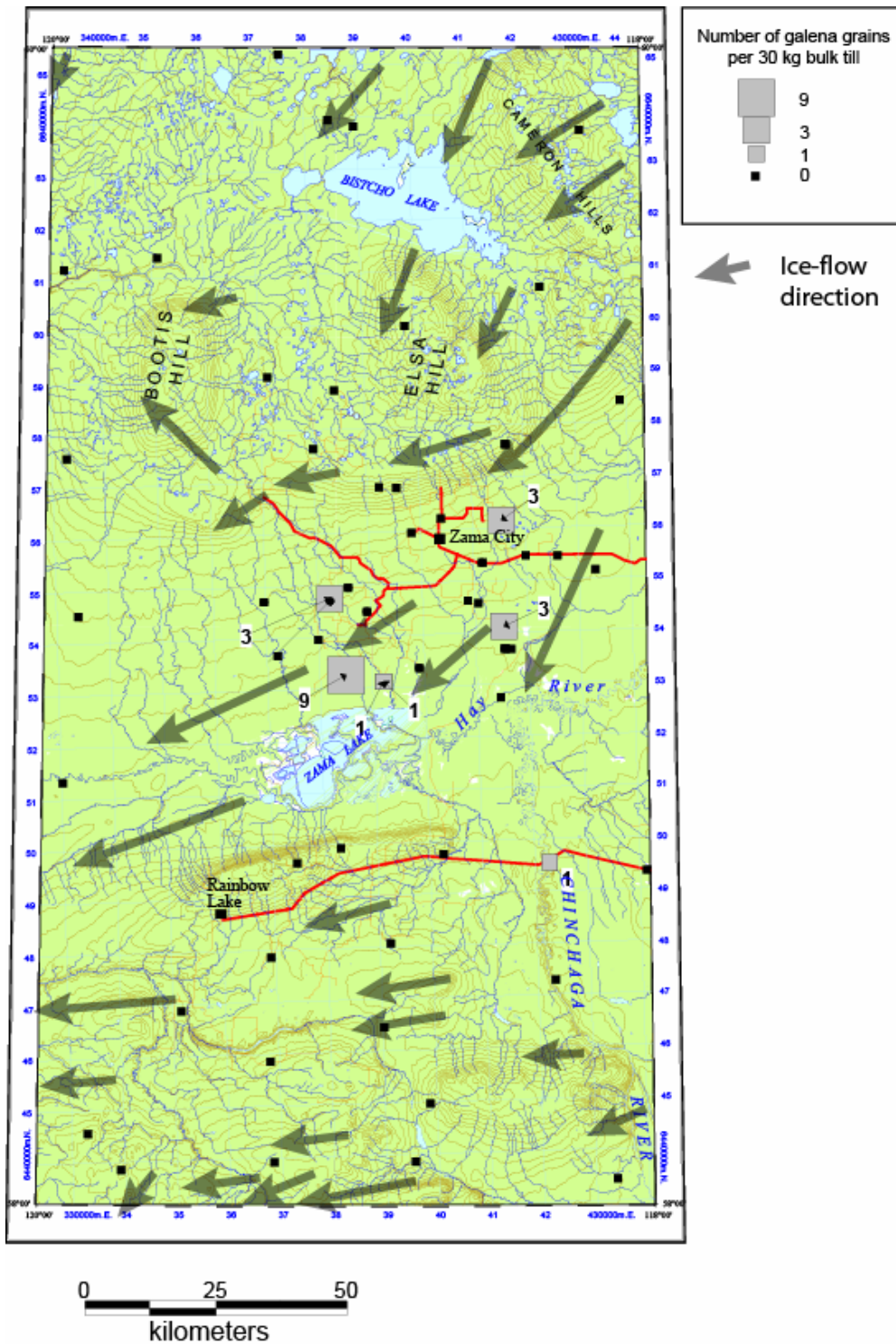


**Figure 14.** (A) Number of galena grains normalized to 30 kg till sample weight. Results are depicted on a topographic map base. Ice-flow directions were obtained from the surficial geology maps (Plouffe et al., 2004, 2006b; Paulen et al., 2005a, 2005b, 2006a, 2006b; Smith et al., 2005b, in press).

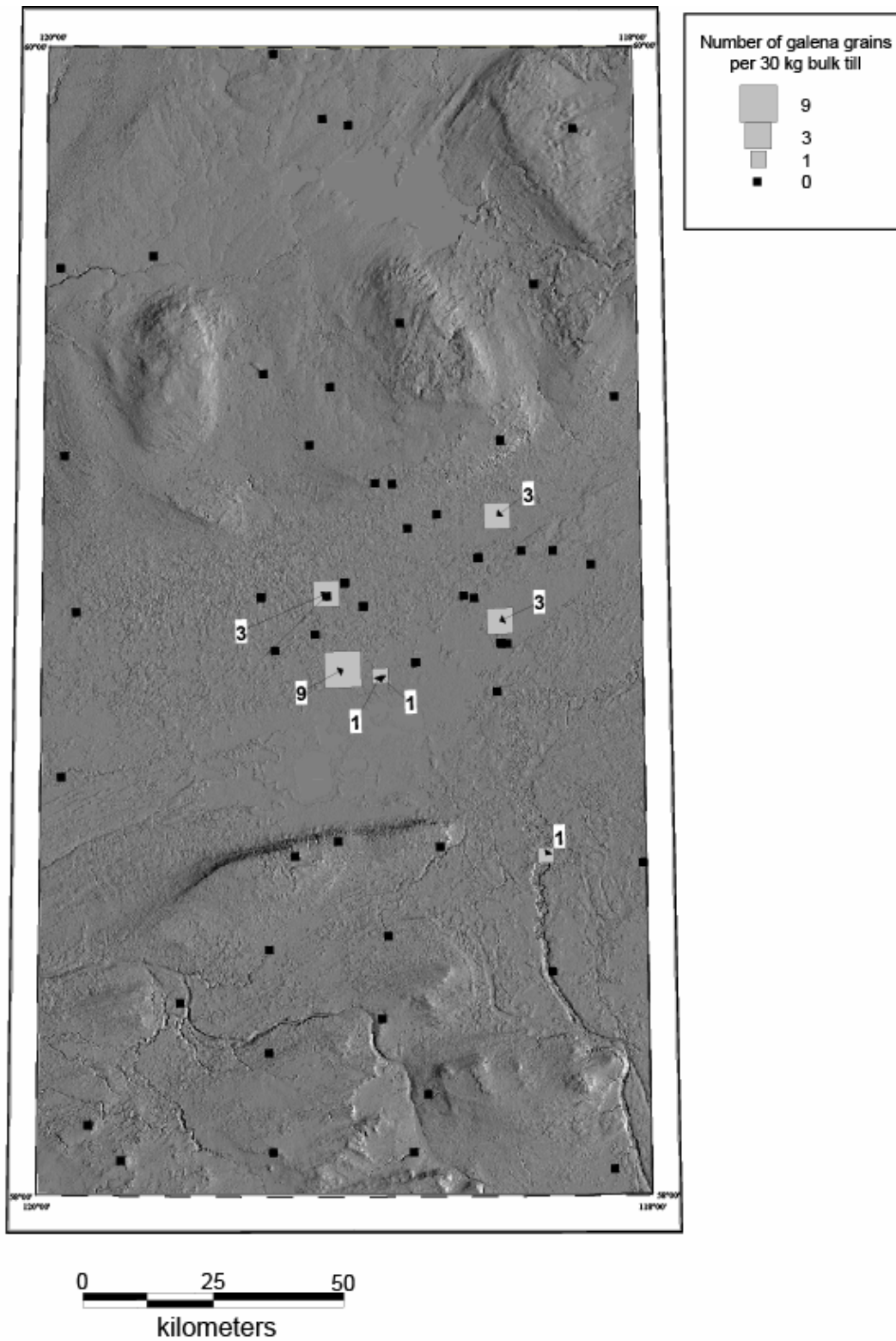


**Figure 14.** (B) Number of galena grains normalized to 30 kg till sample weight. Results are depicted on a digital elevation model.



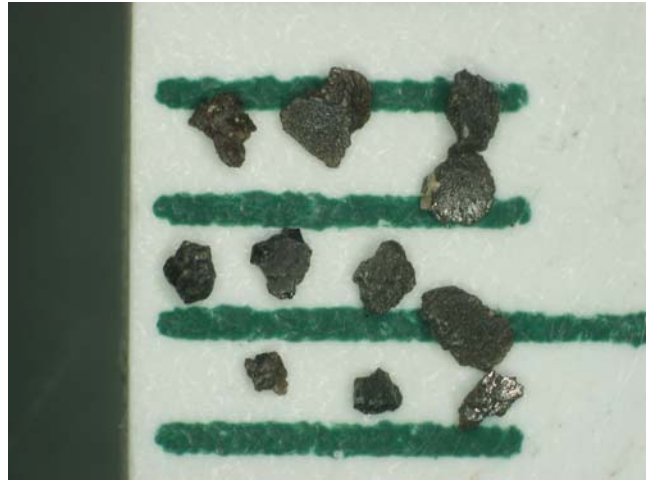
(A)



(B)

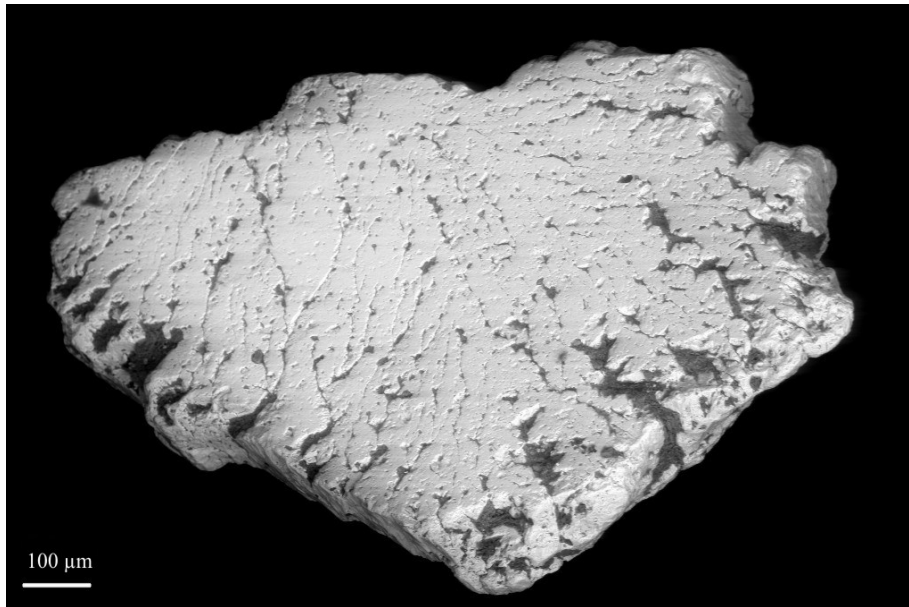


(C)

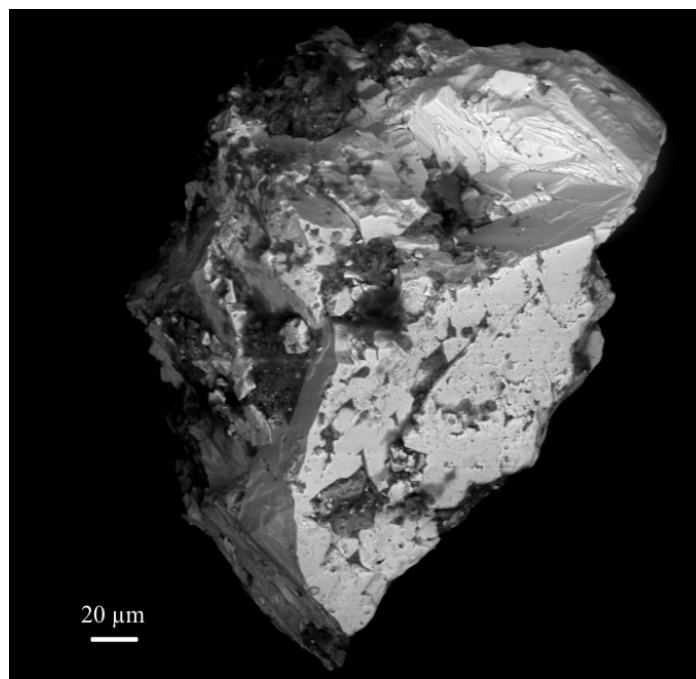


(D)

**Figure 15.** Photographs of sphalerite and galena grains recovered from till samples from NW Alberta; divisions between bars = 1 mm; (A) galena from sample 2290; (B) galena from sample 2929; (C) sphalerite (cleiophane var.) from sample 2396; (D) sphalerite grains from sample 2432; most of the grains recovered from till have the same dark grey to black color.



(A)



(B)

**Figure 16.** Scanning electron microscope (SEM) backscatter images of sphalerite grains recovered from till samples; (A) glacially polished sphalerite grain, (B) angular sphalerite grain with the absence of erosion and polishing which could suggest a short distance of glacial transport.

The average composition of the sphalerite consist of 33.4 wt.% S, 65.4 wt.% Zn, 0.7 wt.% Fe, 0.43 wt.% Cd, and traces amount (0.3 to 0.1 wt %) of Cu, Ag, Se, and In (Appendix 10B). Traces level of Pb and As were detected in a limited number of grains but all thallium (Tl) analyses were below the detection limit of 0.062 wt.%.

	Zn	S	Pb	Fe	Mn	Cu	Cd
<b>Grain periphery (this study)</b>							
Mean (n=135)	65.37	33.42	0.00	0.74	0.00	0.01	0.46
Minimum	63.30	32.56	0.00	0.10	0.00	0.00	0.00
Maximum	66.67	34.15	0.11	3.13	0.02	0.08	1.56
<b>Grain core (this study)</b>							
Mean (n=45)	65.72	33.31	0.00	0.62	0.00	0.01	0.32
Minimum	63.44	32.47	0.00	0.11	0.00	0.00	0.01
Maximum	66.59	34.22	0.10	2.41	0.01	0.05	0.78
<b>Pine Point (Kyle, 1981)</b>							
Mean (n=69)	64.16	33.38	0.21	2.23	0.01	0.02	0.05
Minimum	55.47	31.48	0.00	0.15	0.00	0.00	0.00
Maximum	66.64	33.61	1.05	10.30	0.02	0.16	0.32

**Table 2.** Average and standard deviation of the Zn, Fe, and Cd concentrations in the sphalerite core and grain rim (grain corner) from this study compared with similar data from the Pine Point deposit (Kyle, 1981).

A negative correlation with a  $r^2$  of 0.6 exists between Fe and Zn in sphalerite suggesting a substitution of Fe for Zn in the sphalerite lattice (Fig. 17A). Such negative correlation does not exist between Zn and Cd which might indicate that Cd occurs in small inclusion of other minerals (Fig. 17B). No significant compositional variation was observed between the core and the rims of the sphalerite grains (Table 2). Compared to the composition of sphalerite at the Pine Point deposit (Kyle, 1981), sphalerite from this study contains, on average, lower levels of Pb and Fe, but higher Cd concentrations (Table 2). Furthermore, sphalerite colour from Pine Point varies from tan, yellow, light red-brown, dark red-brown to dark brown (Kyle, 1981). Dark grey sphalerite as observed in till in northwest Alberta was not reported at Pine Point. These observations support the

contention that the sphalerite in till in the Zama Lake – Zama City area is not derived from the Pine Point deposit but rather comes from an unknown mineralized zone.

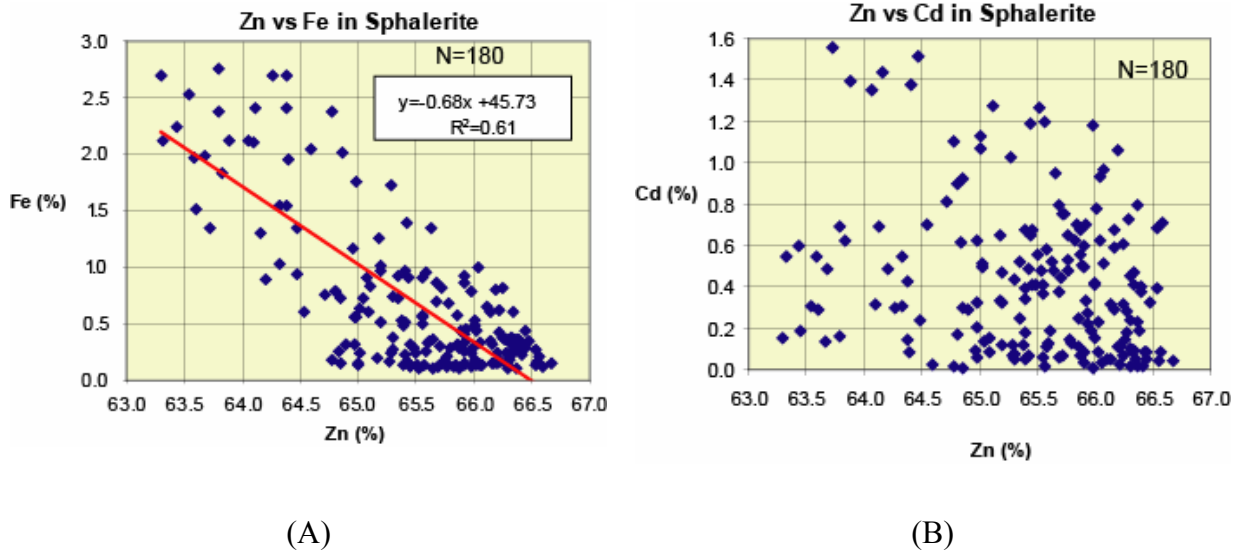


**Figure 17.** Scatter plots of: (A) Fe vs Zn and (B) Cd vs Zn in fifteen sphalerite grains including a total of 180 analyses on grain cores and rims.

### ***On-going research***

As part of the on-going research on the heavy mineral content of glacial sediments and the drift prospecting applications in northwest Alberta, additional bulk glacial sediment samples (dominantly till) are being processed for KIMs and other indicator minerals. These additional samples were collected from NTS map sheets 84 K, L, M, and the western half of N (Fig. 1). Results will be released in joint AGS and GSC Open Files. In addition, Pb and S isotopic analyses are currently being conducted on a number of sphalerite and galena grains recovered from the anomalous till samples collected north of Zama Lake. These new results will also be released in a joint publication. They should provide information as to the potential bedrock source of the sphalerite and galena found in the glacial sediments. The results will be compared with the known data from the Pine Point deposit and other mineralized zones from the surrounding regions (see Nelson et al., 2002).

## **Summary**

Most kimberlite indicator minerals reported by Plouffe et al. (2006a) have been confirmed as such by electron microprobe analyses. In addition, a total of 15 grains originally identified from optical properties alone as low Cr-diopside have been found to contain >0.5 wt.% Cr<sub>2</sub>O<sub>3</sub> and therefore, have been re-classified as KIMs based on the criteria established by Nimis (1998). One grain originally identified as chromite was re-classified as a crustal ilmenite following the electron microprobe analyses. These new data have been compiled in Figures 4 and 5 which depict the distribution of KIMs in till and glaciofluvial sediments in NW Alberta. Out of the 67 till and glaciofluvial samples processed to recover KIMs, 29 contain no KIMs, 35 contain trace amounts (1 to 3 grains) and 3 contain 6 to 9 KIM grains which are considered anomalous concentrations given the low background concentration in all other samples in this study. These results suggest that an unknown kimberlitic source is reflected in the glacial sediments of northwest Alberta.

The new estimates of the number of sphalerite grains in the heavy mineral concentrates confirm the presence of a mineralogical anomaly in glacial sediments from NW Alberta extending from north of Zama Lake to the region of Zama City. The anomaly consists of large concentrations of sphalerite grains with trace amounts of galena. The sphalerite recovered from till has an average concentration of 33.4 wt.% S, 65.4 wt.% Zn, 0.7 wt.% Fe, 0.43 wt.% Cd, and trace amounts (0.3 to 0.1 wt.%) of Cu, Ag, Se, and In.

## **Acknowledgements**

The authors would like to acknowledge M.M. Fenton and J.G. Pawlowicz (Alberta Geological Survey) with whom collaboration has greatly benefited this study. Capable field assistance was provided by T. Ahkhimnachie, L. Andriashek, H. Campbell, C. Kowalchuk, R. Metchooyeah, R. Peterson, M. Tarplee, and J. Weiss. T. Ahkhimnachie and R. Metchooyeah were hired through the Dene Tha' Band Office in Chateh. B. Ward (Simon Fraser University) is thanked for insightful discussions and comments in the field. Paramount Resources Ltd. has kindly provided accommodation to R. Paulen and R. Peterson for field work in the remote region east of Bistcho Lake. G. Prior (Alberta

Geological Survey) selected and submitted the sphalerite grains for electron microprobe analyses. This project was in part funded by the Targeted Geoscience Initiative-2.

## **References**

### **Bostock, H. S.**

1967: Physiographic regions of Canada; Geological Survey of Canada, Map 1254A, map scale 1:5 000 000.

### **Dawson, J. B. and Stephens, W. E.**

1975: Statistical classification of garnets from kimberlite and associated xenoliths; *Journal of Geology*, v. 83, p. 589-607.

### **Dyke, A. S.**

2004: An outline of North American deglaciation with emphasis on central and northern Canada; *in* Quaternary Glaciations - Extent and Chronology, part II, (eds.) J. Ehlers and P. L. Gibbard; Elsevier, Amsterdam, p. 373-424.

### **Fipke, C. E., Gurney, J. J. and Moore, R. O.**

1995: Diamond exploration techniques emphasising indicator mineral geochemistry and Canadian examples; Geological Survey of Canada, Bulletin 423, 86 p.

### **Friske, P. W. B., Prior, G. J., McNeil, R. J., McCurdy, M. W. and Day, S. J. A.**

2003: National geochemical reconnaissance (NGR) stream sediment and water survey in the Buffalo Head Hills area, northern Alberta (parts of NTS 84B, 84C, 84F and 84G) including analytical mineralogical and kimberlite indicator mineral data from silts, heavy mineral concentrates and waters; Alberta Energy and Utilities Board, Alberta Geological Survey, Special Report 66 / Geological Survey of Canada, Open File 1790, 1 CD ROM.

### **Grütter, H. S., Gurney, J. J., Menzies, A. H. and Winter, F.**

2004: An updated classification scheme for mantle-derived garnet, for use by diamond explorers; *Lithos*, v. 77, p. 841-857.

### **Gurney, J. J.**

1984: A correlation between garnets and diamonds in kimberlites; *in* Kimberlite Occurrence and Origin: a Basis for Conceptual Models in Exploration, (eds.) J. E. Glover and P. G. Harris; Geology Department and University Extension, University of Western Australia, Publication No. 8, p. 143-166.

### **Haggerty, S. E.**

1975: The chemistry and genesis of opaque minerals in kimberlites; *in* Physics and chemistry of the Earth, (ed.) A. J. Erlank; Pergamon Press, Volume 9, Oxford, p. 295-307.

**Hutchison, M. T., Nixon, P. H. and Harley, S. L.**

2004: Corundum inclusions in diamonds - discriminatory criteria and a corundum compositional dataset; *Lithos*, v. 77, p. 273-286.

**Kowalchuk, C. J., Ward, B. C., Paulen, R. C. and Plouffe, A.**

2006: Surficial geology, Moody Creek (84M/02), Alberta; Geological Survey of Canada, Open File 5283, Alberta Energy and Utilities Board, Alberta Geological Survey, Map 397, map scale 1:50 000.

**Kyle, J. R.**

1981: Geology of the Pine Point lead-zinc district; in *Handbook of Strata-Bound and Stratiform Ore Deposits*, (ed.) K. H. Wolf; Elsevier, Volume 9, part III, Chapter 11, Amsterdam, p. 643-741.

**Mathews, W. H.**

1980: Retreat of the last ice sheets in northeastern British Columbia and adjacent Alberta; Geological Survey of Canada, Bulletin 331, 22 p.

**Nelson, J., Paradis, S., Christensen, J. and Gabites, J.**

2002: Canadian Cordilleran Mississippi valley-type deposits: a case for Devonian-Mississippian back-arc hydrothermal origin; *Economic Geology*, v. 97, p. 1013-1036.

**Nimis, P.**

1998: Evaluation of diamond potential from the composition of peridotitic chromian diopside; *European Journal of Mineralogy*, v. 10, p. 505-519.

**Okulitch, A.**

2006: Bedrock geology, Peace River, Alberta; Geological Survey of Canada, Open File 5282, map scale 1:1 000 000.

**Paulen, R. C., Fenton, M. M., Pawlowicz, J. G., Smith, I. R. and Plouffe, A.**

2005a: Surficial Geology of the Little Hay River Area, Alberta (NTS 84L/NW); Alberta Energy and Utilities Board, EUB/AGS Map 315, map scale 1:100,000.

**Paulen, R. C., Fenton, M. M., Weiss, J. A., Pawlowicz, J. G., Plouffe, A. and Smith, I. R.**

2005b: Surficial Geology of the Hay Lake Area, Alberta (NTS 84L/NE); Alberta Energy and Utilities Board, EUB/AGS Map 316, map scale 1:100,000.

**Paulen, R. C., Kowalchuk, C. J., Plouffe, A., Ward, B. C. and Smith, I. R.**

2006a: Surficial Geology of the Zama City Area (NTS 84M/SE); Alberta Energy and Utilities Board, EUB/AGS Map 361 and Geological Survey of Canada, Open File 5184, map scale 1:100 000.

**Paulen, R. C., Plouffe, A. and Smith, I. R.**

2006b: Surficial Geology of the Beatty Lake Area (NTS 84M/NE); Alberta Energy and Utilities Board, EUB/AGS Map 360 and Geological Survey of Canada, Open File 5183, map scale 1:100 000.

**Pawlowicz, J. G., Hickin, A. S., Nicol, T. J., Fenton, M. M., Paulen, R. C., Plouffe, A. and Smith, I. R.**

2005a: Bedrock topography of Zama Lake area (NTS 84L), Alberta; Alberta Energy and Utilities Board, EUB/AGS Map 328, map scale 1:250 000.

**Pawlowicz, J. G., Hickin, A. S., Nicol, T. J., Fenton, M. M., Paulen, R. C., Plouffe, A. and Smith, I. R.**

2005b: Drift thickness of Zama Lake area (NTS 84L), Alberta; Alberta Energy and Utilities Board, EUB/AGS Map 329, map scale 1:250 000.

**Pawlowicz, J. G., Nicoll, T. J. and Sciarra, J. N.**

in press-a: Bedrock topography of Bistcho Lake area (NTS 84M), Alberta; Alberta Energy and Utilities Board, EUB/AGS Map 416, map scale 1:250 000.

**Pawlowicz, J. G., Nicoll, T. J. and Sciarra, J. N.**

in press-b: Drift thickness of Bistcho Lake area (NTS 84M), Alberta; Alberta Energy and Utilities Board, EUB/AGS Map 417, map scale 1:250 000.

**Plouffe, A., Paulen, R. C. and Smith, I. R.**

2006a: Indicator mineral content and geochemistry of glacial sediments from northwest Alberta (NTS 84L, M): new opportunities for mineral exploration; Ottawa, Geological Survey of Canada, Open File 5121, Alberta Energy and Utilities Board, Alberta Geological Survey, Special Report 77, 1 CD-ROM.

**Plouffe, A., Paulen, R. C. and Smith, I. R.**

2006b: Surficial geology, Thinahtea Creek, Alberta (NTS 84 M/NW); Geological Survey of Canada, Open File 5070, Alberta Energy and Utilities Board, Alberta Geological Survey Map 395, map scale 1:100 000.

**Plouffe, A., Smith, I. R., Paulen, R. C., Fenton, M. M. and Pawlowicz, J. G.**

2004: Surficial geology, Bassett Lake, Alberta (NTS 84L SE); Geological Survey of Canada, Open File 4637, map scale 1:100 000.

**Smith, I. R., Paulen, R. C. and Plouffe, A.**

in press: Surficial geology, Mega River, Alberta (NTS84 M/SW); Geological Survey of Canada, Open File 5237, Alberta Energy and Utilities Board, Alberta Geological Survey, Map 396, map scale 1:100 000.

**Smith, I. R., Paulen, R. C., Plouffe, A., Kowalchuk, C. and Peterson, R.**

2005a: Surficial mapping and granular aggregate resource assessment in northwest Alberta; *in* Summary of Activities 2005, British Columbia Ministry of Energy and Mines, Victoria, p. 80-95.

**Smith, I. R., Plouffe, A., Paulen, R. C., Fenton, M. M. and Pawlowicz, J. G.**

2005b: Surficial geology, Hay River, Alberta (NTS 84L/SW); Geological Survey of Canada, Open File 4754, map scale 1:100 000.

**Sobolev, N. V.**

1977: Deep seated inclusions in kimberlites and the problem of the composition of the upper mantle; American Geophysical Union, Washington, 279 p.

**Wyatt, B. A., Baumgartner, M., Anckar, E. and Grutter, H.**

2004: Compositional classification of "kimberlitic" and "non-kimberlitic" ilmenite; Lithos, v. 77, p. 819-840.